Journal of the European Ceramic Society 22 (2002) 2093–2100

www.elsevier.com/locate/jeurceramsoc

Direct synthesis of PMN samples by spray-drying

A.L. Costa*, C. Galassi, E. Roncari

CNR-IRTEC, Research Institute for Ceramics Technology, Via Granarolo 64, Faenza, I-48018 Italy

Received 27 June 2001; received in revised form 28 December 2001; accepted 6 January 2002

Abstract

The processing and characterisation of $Pb(Mg_{1/3}Nb_{2/3})O_3$ (PMN) materials, obtained either by spray-drying the solution of the precursors or by the conventional "columbite" method, were investigated and the morphological and micro-structural characteristics were compared. The acid solution of ammonium-peroxo-niobium complex, magnesium and lead nitrates was spray-dried and the precursor powder obtained was calcined at different temperatures ranging from 350 to 900 °C. The morphologies and the XRD patterns of the powders were compared. The calcined powders exhibited a pyrochlore phase above 400 °C converting into an almost pure perovskite phase at 800 °C. The powder calcined at 350, 500 and 800 °C were sintered at different temperatures, ranging from 950 to 1150 °C, always resulting in a pure perovskite PMN material. The XRD patterns of as-fired surfaces of samples sintered at 950 and 1050 °C showed an unwanted PbO phase together with the main PMN, nevertheless this secondary phase is not present in the ground surfaces. The high reactivity of sprayed powder is reflected in the formation and densification of pure perovskite PMN material with a faster process as regards the conventional one; in particular samples of about 96% theoretical density were obtained starting from the amorphous powder calcined at low temperature (350 °C) through a reaction sintering process. Furthermore, due to the better flowability of the spray-dried powder, the cold consolidation process is highly improved and no binder addition to powder is necessary.

Keywords: Chemical processing; Microstructure; Pb (Mg; Nb) O_3; PMN; Spray-drying

1. Introduction

Lead magnesium niobate ceramics, $Pb(Mg_{1/3}Nb_{2/3})O_3$ (PMN) and related compounds, are the most widely studied lead-based relaxor ferroelectric materials, because of their excellent dielectric and electrostrictive properties, making them very promising candidates for applications such as multilayer capacitors, sensors and actuators.[1]

The main problem in the fabrication of pure perovskite PMN samples is the formation of the unwanted pyrochlore phase that decreases the dielectric and electromechanical performances of the material. In two studies regarding the formation and the stability of the perovskite and pyrochlore compounds in the system PbO–MgO–Nb_2O_5, Guha[2,3] demonstrated the subsolidus compatibility relationships among the cubic perovskite phase [$Pb(Mg_{1/3}Nb_{2/3})O_3$], PbO, MgO and pyrochlore that was identified as a cubic oxygen-deficient ternary phase with a general formula $Pb_{2-x}(Mg_{0.286}Nb_{1.714})O_{6.571-x}$, where $0 > x > 0.286$. The pyrochlore phase is the major product at the initial stages of the solid-state reactions between the three constituent oxides, owing to the preferential reaction between Nb_2O_5, a large amount of PbO and a small amount of MgO. With the increasing reaction temperature and time, pyrochlore further combines with the remaining PbO and MgO to yield the perovskite PMN.[2,4] The residual pyrochlore phase, together with the main perovskite, is a consequence of low MgO reactivity and intrinsic inhomogeneity of the reacting mixture. Furthermore, the heating treatment at temperatures above 800 °C can lead to the formation of pyrochlore phase as a consequence of PbO loss by evaporation, if samples are not fired in a saturated PbO atmosphere.[4–6] The reaction between the precalcined columbite ($MgNb_2O_6$) phase and the PbO[7] bypasses the direct formation of pyrochlore, even if its formation can anyway come from PMN decomposition during sintering. The purity degree of the raw materials and the homogeneity of the precursor mixture influence the final stoichiometry of PMN ceramics also in the case of columbite method.

* Corresponding author.
E-mail address: acosta@racine.ra.it (A.L. Costa).

0955-2219/02/$ - see front matter
PII: S0955-2219(02)00026-2

Unreacted or slightly deficient MgO during the formation of columbite let some Nb_2O_5 free to react with PbO in the following calcination step with the consequent formation of pyrochlore often coexisting with a PbO-rich grain boundary phase.[4] In the case of unreacted MgO, it will also be possible to find some MgO inclusions inside the PMN primary phase.[8,9] Furthermore, it was evidenced that the small amount of pyrochlore into the starting calcined powders can promote different sintering mechanisms leading to very different microstructures and final properties of the samples even if the pyrochlore phase, located on the surface, is removed.[9] Several processes were investigated to eliminate or reduce the pyrochlore phase, including either the modification of the mixed oxide procedure, such as the "columbite" method,[7] or wet chemical processes, such as chemical precipitation (coprecipitation,[10] stepwise precipitation[11,12] partial oxalate route[13,14]), sol-gel[15–21] and citrate routes,[22] freeze-drying[12,23] and spray-pyrolysis[24] methods. The main feature of the wet chemical processes is the mixing of the reagents at a molecular level that leads to a strong improvement of reactivity of the precursor powders. The enhancement of reactivity is particularly important for the PMN system where incomplete reactions between components involve the formation of parasite secondary phases.

Among wet chemical techniques a distinction should be made between direct synthesis from solution (DSS),[23] like freeze-drying and spray-pyrolysis methods, and chemical routes involving a precipitation process from organic or inorganic solution such as co-precipitation, sol-gel and citrate routes. In the last mentioned cases, the process of separation of precursors from the solution can be influenced by the different solubility or hydrolysis rates of the components that can give rise to selective precipitation. In the DSS methods the precipitation of components, consequent to the solvent evaporation, takes place inside the droplets, ensuring a control of stoichiometry at this level. Together with a better control of stoichiometry, DSS methods produce finer particles ensuring a better powder sinterability.

Although the spray-drying is commonly applied to water-based ceramic suspensions for the powders atomisation,[25] its application to solutions is especially useful in the preparation of multicomponent ceramic powders whose properties are strongly dependent on chemical homogeneity.[26] Unlike spray-pyrolysis, where the solution is dried and precursor directly pyrolized inside the reaction chamber, the spray-drying process atomises the solution producing an amorphous powder which is calcined in a further step. The spray-drying of solutions is a DSS method never used before to obtain PMN powders. In comparison to other solution techniques, the spray-drying process is quite simple and permits a good theoretical simulation of experimental parameters, to optimise the process.

In the present study, the phase formation, the particle morphology and the densification behaviour of powders obtained by spray-drying of solutions were investigated. The advantages of this new process route were evaluated in comparison with the conventional "columbite" route to produce PMN materials.

2. Experimental

2.1. Synthesis and characterisation of powders

An aqueous nitrate solution containing Pb^{2+}, Mg^{2+} and Nb^{5+} cations in the mole ratio of 3:1:2 was prepared using Nb-ammonium complex AD/1440 (Nb_2O_5 25.6%, CBMM-Companhia Brasileira de Metalurgia e Mineração), $Mg(NO_3)_2{\cdot}6H_2O$ (99.5%, Fluka), $Pb(NO_3)_2$ (99%, Fluka) as precursor reagents. The niobium and magnesium precursors were first dissolved in a nitric acid solution (3 M, Carlo Erba Reagenti) adding hydrogen peroxide (Carlo Erba Reagenti) to reach the final molar ratio hydrogen peroxide : niobium = 2. The addition of hydrogen peroxide promotes the solubility of hydrated niobia forming more soluble yellow peroxo-niobium complexes.[5] A nitric acid solution (2 M) of lead nitrate was added dropwise to the niobium and magnesium solution. The as prepared solution, kept under stirring, was sprayed and dried in the laboratory spray drier (Mod. SD-05, Lab-Plant Ltd., Huddersfield, England) at fixed process parameters: pump suction flow 168 cm^3/h, air flow 68 m^3/h, atomising air pressure 2.2 bar, nozzle diameter 0.5 mm, air stream temperature 220 °C.

The chemical composition of dried powder was determined by inductively coupled plasma–optical emission spectrometry (ICP–OES) (Liberty 200, Varian, Clayton South, Australia). Samples were calcined in a covered alumina crucible in the 350–900 °C temperatures range with a heating rate of 100 °C/h and a fixed soaking time of 1 h. The thermogravimetry (TGA) and differential thermal analyses (DTA) were carried out on the powder as-sprayed and calcined at 350 °C at a heating rate of 20 °C /min with a simultaneous thermal analyser (STA 409, Netzsch, Selb/Bavaria, Germany); the dilatometric analysis was performed at a heating rate of 5 °C/min up to 1000 °C with a dilatometer (402 E, Netzsch, Selb/Bavaria, Germany). The phases formed during the heating treatment were identified by a powder X-ray diffractometer (XRD) (Miniflex Rigaku, Japan) operating with Ni-filtered CuK_α radiation; 2ϑ angles from 20 to 70° were explored. The particle size distribution was measured by X-ray sedimentation technique (Sedigraph 5100, Micromeritics, Norcross, GA) and the specific surface area was determined by BET single point method (Sorpty 1750, Carlo Erba, Milano, Italy). Powder morphology

was observed by scanning electron microscopy (SEM) (Stereoscan 360, Leica, Cambridge, UK).

2.2. Preparation and characterisation of sintered PMN

The powders calcined at 350 °C (A), 500 °C (B) and 800 °C (C) were dry ground using an agate mortar, sieved through a 100-mesh sieve and directly pressed into disks (12 mm in diameter and 2 mm thick) by die pressing at 125 MPa, followed by isostatic pressing at 300 MPa. The disks were then supported on ZrO_2 setters, covered with an alumina crucible, sealed with $PbZrO_3$ (PZ) powder to minimise the PbO volatilisation. The sintering process was performed in air at different temperatures (950–1150 °C) with the same soaking time of 1 h. The density of the sintered samples was determined by the Archimedes method in deionised water. The microstructure of the polished fracture surfaces was investigated by SEM coupled with an energy-dispersive X-ray spectrometer (EDS). The average grain size was measured from the micrographs using a linear intercept technique. The phases present on as-fired and ground surfaces were analysed using the X-ray diffractometer. In order to make a comparison with samples obtained by spray-drying route (SD), PMN samples with the same stoichiometric composition and dimensions were prepared by the conventional "columbite" solid state reaction from the oxides[3] (C-MMO). Reagent-grade starting powders of PbO (99.99%, Aldrich), Nb_2O_5 (99.99%, Aldrich) and pre-dried (800 °C for 1 h) MgO (99%, Carlo Erba Reagenti) were used as raw materials. The procedure adopted to prepare PMN samples through the spray-drying and the "columbite" methods are shown in Figs. 1 and 2, respectively. The spray-drying method includes less

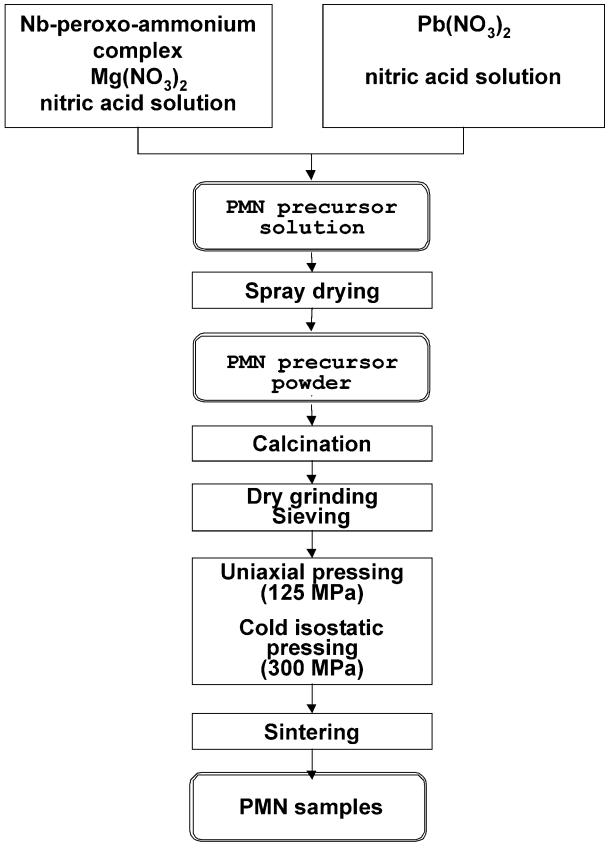

Fig. 1. Flow diagram for the preparation of PMN samples through the spray-drying route.

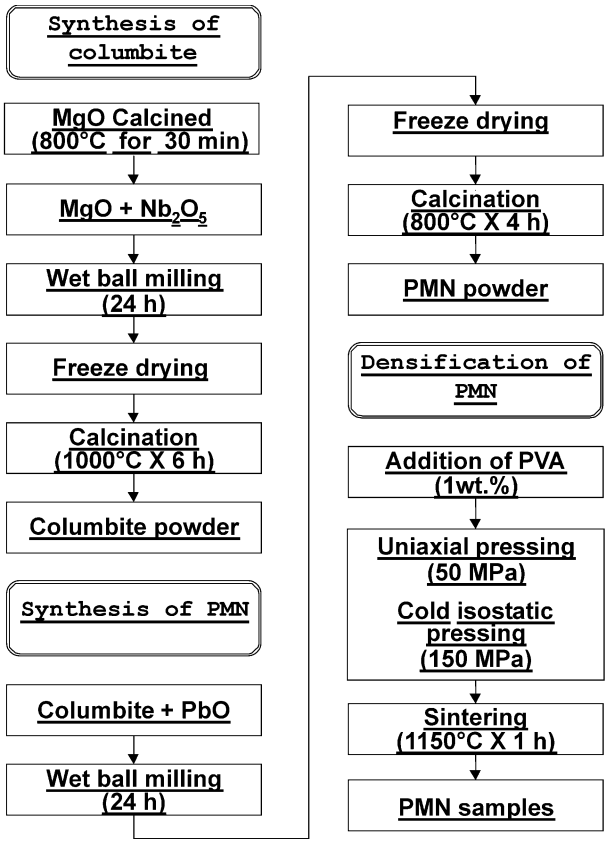

Fig. 2. Flow diagram for the preparation of PMN samples through the "columbite" mixed oxide route.

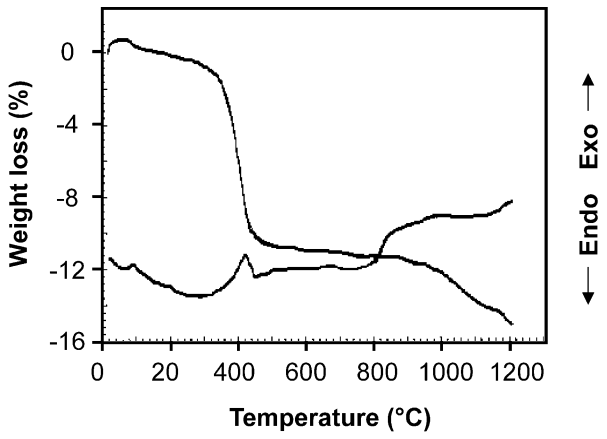

Fig. 3. DTA and TGA of SD powder calcined at 350 °C.

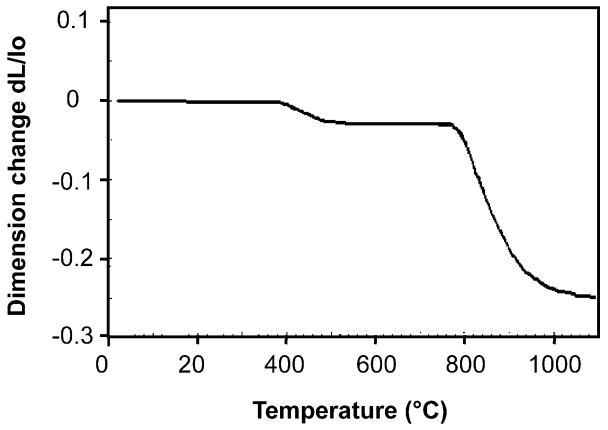

Fig. 4. Dilatometric analysis of as-die-pressed sample of SD powder calcined at 350 °C.

steps than the conventional "columbite" route and only one calcination step is required.

3. Results and discussion

3.1. Precursor powder

From the results of the ICP–OES analysis, the stoichiometry of the sprayed precursor powders corresponds to the nominal value, with differences lying within the experimental error. The DTA analysis of the as-sprayed powder showed two big exothermic peaks around 300 °C, referred to magnesium nitrate and niobium ammonium complex decomposition, corresponding to a big weight loss in the TGA analysis that makes less detectable the smaller peaks referred to the other

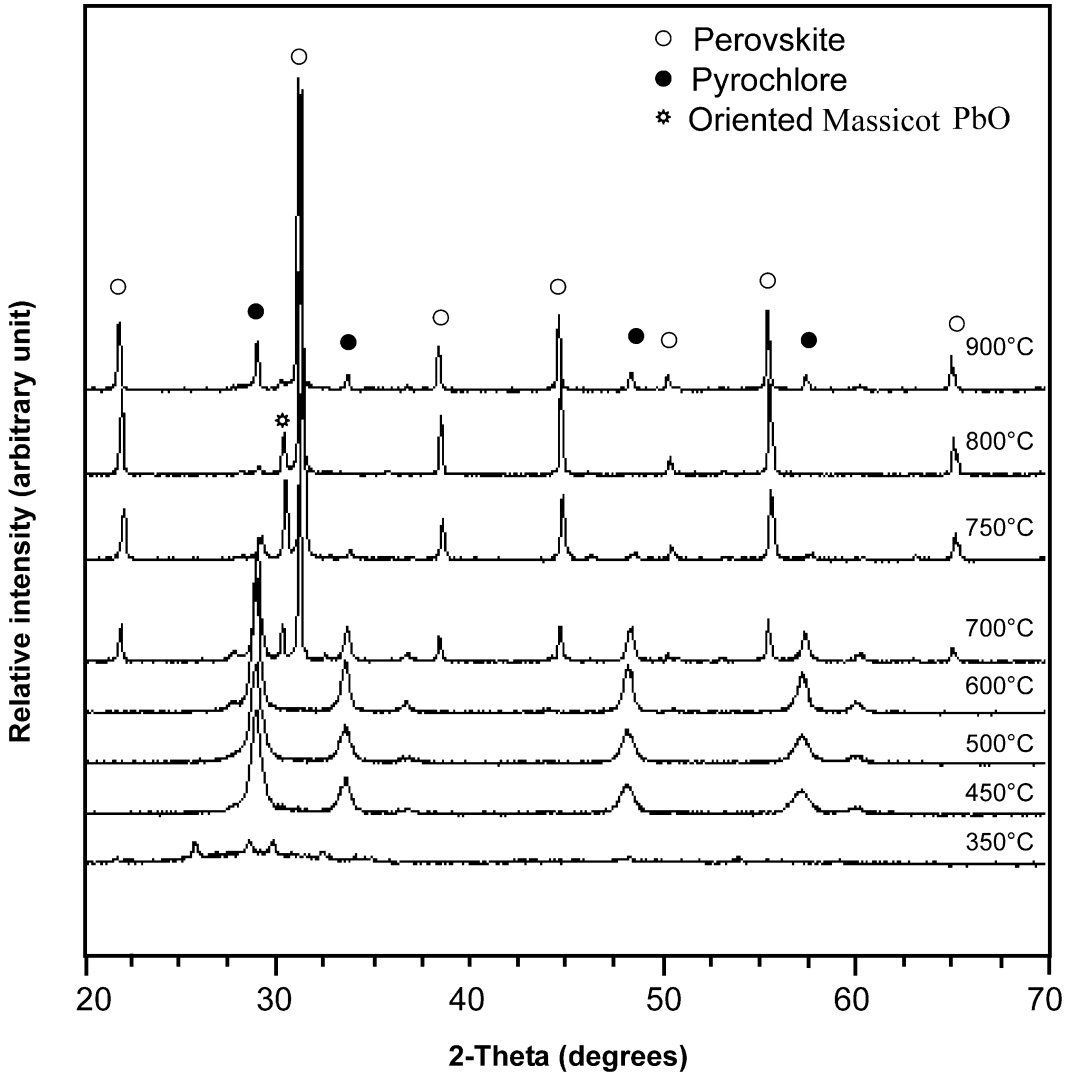

Fig. 5. XRD patterns of SD powder calcined for 1 h at different temperatures.

transformations. For this reason only the thermal and dilatometric analysis of powder calcined at 350 °C are shown in Figs. 3 and 4, respectively. Considering that magnesium nitrate and niobium ammonium complex are just decomposed into the corresponding oxides during the calcination process at 350 °C, the exothermic peak associated to a weight loss of 10%, in the 400–440 °C temperature range is attributed to the lead nitrate decomposition. The endothermic peak at 460 °C can be attributed to pyrochlore formation, as XRD analysis confirms. The transformations occurring above 750 °C may be attributed to the formation and partial evaporation (weight loss about 2 wt.% up to 1100 °C) of a PbO rich liquid phase that drives to the completion of the perovskite formation,[27] coherent with a ternary eutectic liquid phase formed by perovskite, pyrochlore and unreacted PbO.[2] The PbO rich liquid phase will result in a crystallised PbO phase upon cooling, as XRD analysis confirms. The appearance of this phase can be connected to the mechanism of sintering and shrinkage that takes place starting from 800 °C (Fig. 4). The phase evolution, recorded by XRD analysis, at increasing temperature is shown in Fig. 5. The XRD patterns evidence the formation of the pyrochlore phase at 450 °C and the formation of the perovskite phase together with pyrochlore and unreacted PbO in the 700–800 °C temperature range. The PbO and pyrochlore phases are almost completely transformed into the perovskite phase at 800 °C, while above 800 °C, the PbO partially evaporates and the pyrochlore phase is formed again. The SEM morphologies of the SD powder as-sprayed and calcined at various temperatures are shown in Fig. 6. The spherical hollow particles obtained after the spray-drying process shrink during the calcination to form denser and smaller aggregates. The specific surface area and particle sizes of SD powders, calcined at 350 °C (SD-A) and 800 °C (SD-C) are reported in Table 1 together with data of conventional powder calcined at 800 °C (C-MMO). The enhanced reactivity of powder SD-A is confirmed by the presence of nanosize primary particles forming large aggregates (about 7 μm). The spray-dried powder starts to sinter during the calcination at 800 °C (SD-C), as confirmed by morphology shown in Fig. 6, and by the reduction of the specific surface area to half of that of powder C-MMO, calcined at the same temperature.

Table 1
Specific surface area and mean particle diameter of powders

Powder	S.s.a. (m^2/g)	Agglomerate size (μm)	Primary particles size* (μm)
C-MMO	1.2	1.56	0.61
S-D (A)	4.7	7.03	0.16
S-D (C)	0.5	2.09	1.45

* Primary particle diameter = $6/(\rho_{the} \cdot s.s.a)$, theoretical density = 8.13 g/cm^3 (ρ_{the}).

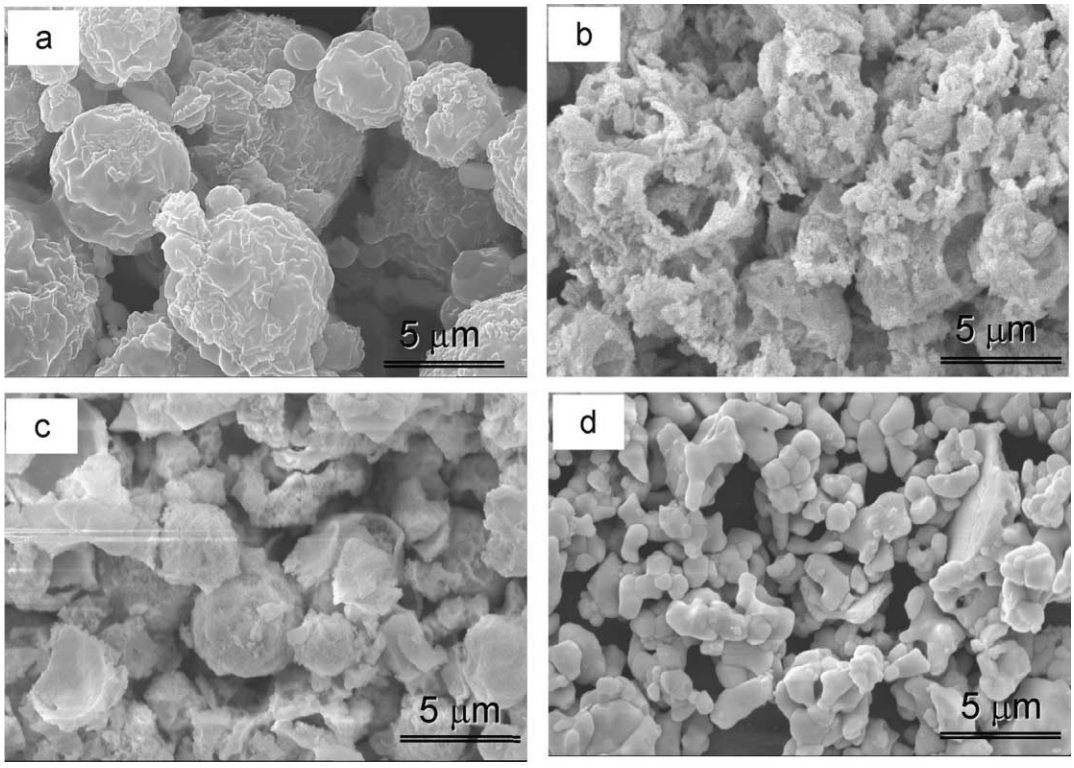

Fig. 6. SEM morphologies of SD powder: (a) as sprayed, (b) SD-A, (c) SD-B and (d) SD-C calcined at 350,500 and 800 °C, respectively.

3.2. Sintering

The values of green density, shrinkage and sintered density of samples sintered at 950, 1050 and 1150 °C are shown in Table 2. The green density of samples obtained from spray-dried powders increases with the calcination temperature, reaching a 79% relative density in the case of powder SD-C, calcined at 800 °C. This is a consequence of the high reactivity of the as sprayed powder that results partially sintered already at 800 °C. The corresponding final sintered densities for powders SD-A and SD-C are almost comparable and generally lower than those of C-MMO samples. The sintered densities of SD samples increase with sintering temperature even if there are actually small differences between samples sintered at 1050 and 1150 °C. The most relevant result is related to samples sintered at 1050 °C from powder SD-A, calcined at 350 °C. As the starting powder is amorphous, the densification takes place simultaneously to the formation of the perovskite phase through a reaction sintering mechanism. The final density (7.8 g/cm^3) is comparable with that of C-MMO sample sintered at 100 °C higher temperature, starting from a powder calcined at 800 °C. The XRD patterns of as-fired SD samples sintered at different temperatures are shown in Fig. 7. An oriented massicot PbO phase was revealed, together with the PMN perovskite phase, in samples sintered at 950 and 1050 °C. This secondary phase is present only in the first few microns under the surface and disappears at 1150 °C. The SEM morphologies of the polished and thermally etched surface as-sintered and upon grinding are shown in Fig. 8 (a) and (b), respectively. The grinding treatment (grinding depth: 150 μm) is enough to remove PbO crystallised on the as-fired surface. This surface PbO phase can derive from the formation and migration toward the surface of a PbO rich liquid phase[28] that crystallises upon cooling on the surface of samples sintered at 950 and 1050 °C. The absence of PbO in the samples sintered at 1150 °C is due to the higher evaporation rate. An example of PMN phase stabilisation without a fixed stoichiometry

Table 2
Green density, shrinkage and sintered density of samples sintered at different temperatures

Powder	S.s.a. (m^2/g)	Sintered density (g/cm^3)			Shrinkage (%)[a]		
		950 °C	1050 °C	1150 °C	950 °C	1050 °C	1150 °C
C-MMO	58			8.0			15.8
SD-A	50	7.6	7.8	7.8	20.6	21.2	21.5
SD-B	57	7.4	7.5	7.6	14.3	14.6	15.2
SD-C	79		7.8	7.9		6.7	7.0

[a] Shrinkage (%) = [1(green body)-1(sintered body)/1(green body)] × 100.

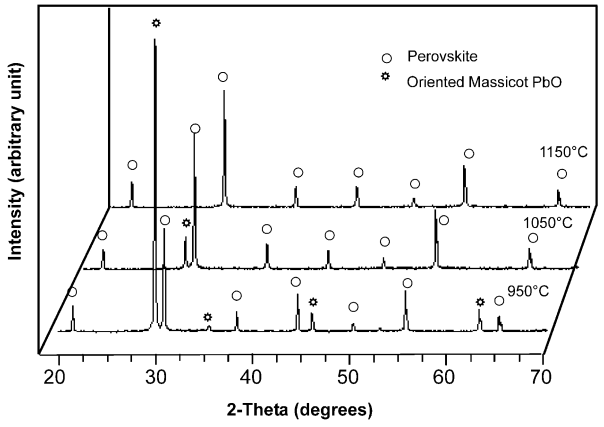

Fig. 7. XRD patterns of as-fired surface (SD samples sintered for 1 h at different temperatures).

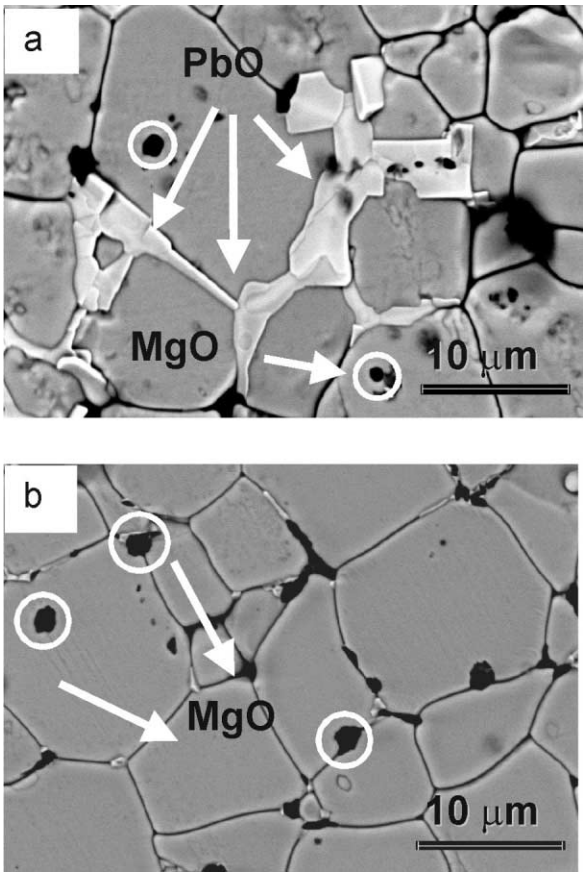

Fig. 8. SEM morphologies of polished and thermally etched surfaces of SD samples sintered at 1050 °C for 1 h: (a) as fired; (b) ground.

Table 3
Mean grain size (μm) of samples sintered at different temperature

Powder	950 °C	1050 °C	1150 °C
C-MMO			4.5
SD-1	7.3	10.9	12.9
SD-B	6.8	10.8	11.4
SD-C			8.7

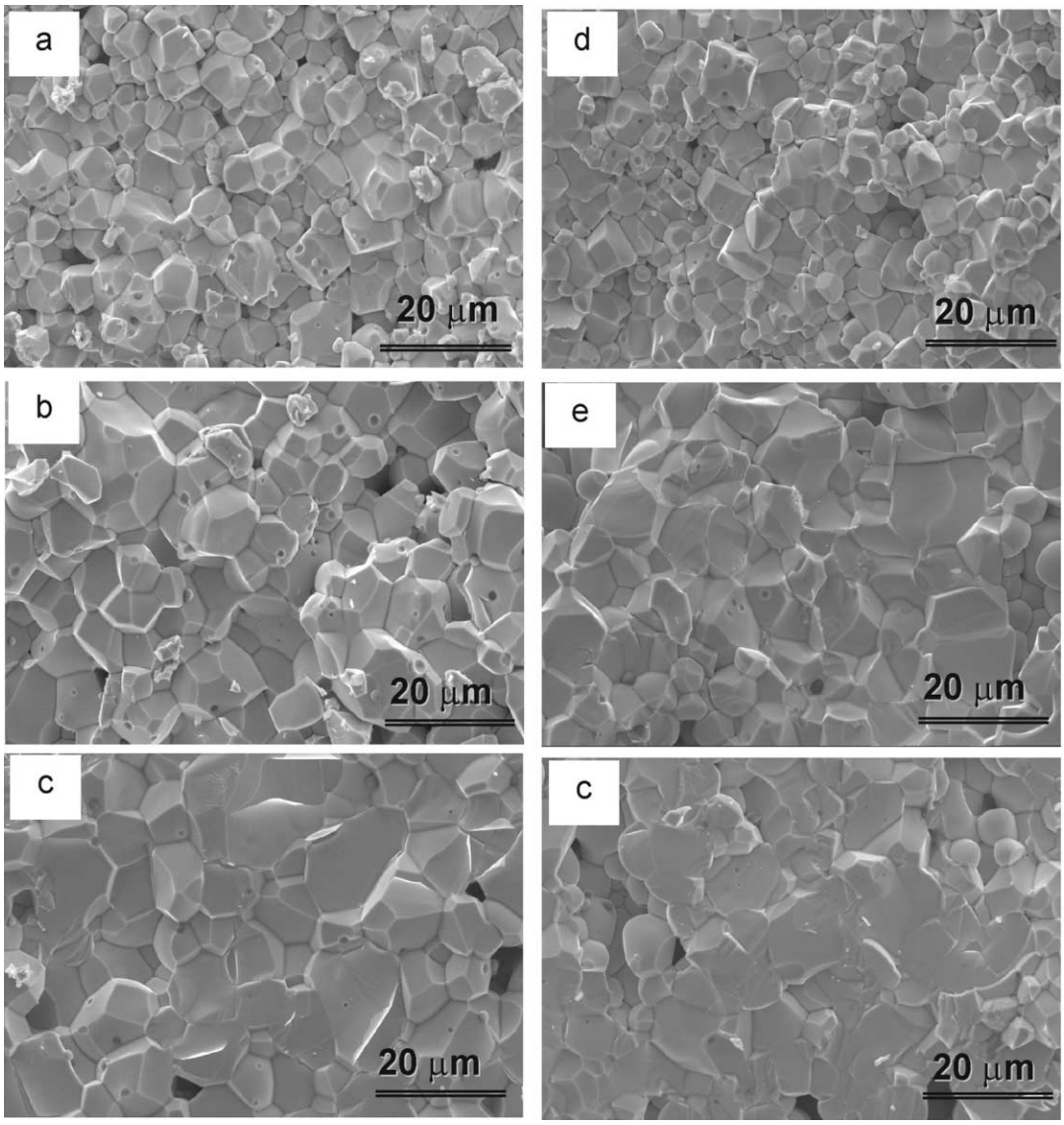

Fig. 9. SEM morphologies of fracture surfaces of samples SD-A, calcined at 350 °C, sintered at 950 °C (a), 1050 °C (b), 1150 °C (c) and SD-B; calcined at 500 °C; sintered at 950 °C (d), 1050 °C (e) and 1150 °C (f).

was given by Beltran et al.[19] The formation of a PbO rich liquid phase is not responsible for increasing density in comparison with samples obtained by solid state reaction from the oxides, nevertheless an investigation of the PbO role in the sintering mechanism is still in progress. The values of mean grain sizes of samples from SD and C-MMO powders are compared in Table 3. The grain sizes of SD samples are two to three times higher than those of C-MMO samples. It is a confirmation of the expected behaviour: the lower the calcination temperature, the higher the reactivity of SD powder. The fracture surfaces of SD samples from powder A and B sintered at various temperatures are shown in Fig. 9. The mean grain size increases as the temperature rises and the fracture changes from intergranular to intragranular.

4. Conclusions

Chemically homogeneous PMN precursor powders are synthesised by spray drying a nitric acid solution of lead and magnesium nitrates, and niobium ammonium complex. Starting from amorphous powder, calcined at 350 °C, PMN samples, in the pure perovskite phase, are sintered to 93–96% relative density at 950–1050 °C. In comparison to the conventional "columbite" method, that implies the synthesis of columbite at 1000 °C followed by the calcination at temperature not lower than 800–850 °C and the sintering at 1150–1200 °C, the spray-drying route allows the synthesis of a pure PMN sample at a lower temperature, through a one step reaction sintering mechanism. This simplified process can be further improved optimising spray-drying conditions

and, as a consequence, precursor powder morphology, in order to obtain an increased final density with homogeneous microstructure.

Acknowledgements

We gratefully acknowledge Dr Elena Landi for thermal analyses, Silvano Tarlazzi for XRD analyses and Dr Alida Bellosi for helpful discussion about sintering mechanism.

References

1. Gupta, S. M. and Kulakarni, A. R., Synthesis and dielectric properties of lead magnesium niobate-a review. *Mater. Chem. Phys*., 1994, **39**, 98–109.
2. Guha, J. P., Reaction chemistry and subsolidus phase equilibria in lead-based relaxor systems: part I. *J. Mater. Sci*., 1999, **34**, 4985–4994.
3. Guha, J. P., Reaction chemistry and subsolidus phase equilibria in lead-based relaxor systems: part II. *J. Mater. Sci*., 2001, **36**, 5219–5226.
4. Bouquin, O. and Lejeune, M., Formation of the perovskite phase in the $Pb(Mg_{1/3}Nb_{2/3})O_3$–$PbTiO_3$ system. *J. Am. Ceram. Soc*., 1991, **74**(5), 1152–1156.
5. Paik, D. S. and Komarneni, S., Composites of $0.9Pb(Mg_{1/3}Nb_{2/3})O_3$–$0.1PbTiO_3$ prepared by a sol-gel method: effect of atmosphere powders. *J. Mater. Sci*., 1999, **34**, 2313–2317.
6. Supon, A. and Noel, W. T., Relationships between sintering conditions, microstructure and dielectric properties of lead magnesium niobate. *J. Eur. Ceram. Soc*., 1999, **82**(11), 3075–3079.
7. Swartz, S. L. and Shrout, T. R., Fabrication of perovskite lead magnesium niobate. *Mater. Res. Bull*., 1982, **17**, 1245–1250.
8. Goo, E. and Okazaki, K., Microstructure of lead-magnesium niobate ceramics. *J. Am. Ceram. Soc*., 1986, **69**(8), C188–C190.
9. Costa, A. L., Fabbri, G., Roncari, E., Capiani, C. and Galassi, C., Pyrochlore phase and microstructure development in lead magnesium niobate materials. *J. Eur. Ceram. Soc*., 2001, **21**(9), 1165–1170.
10. Watanabe, A., Haneda, H., Moriyoshi, Y., Shirasaki, S., Kuramoto, S. and Yamamura, H., Precipitation of lead magnesium niobate by a coprecipitation method. *J. Mater. Sci*., 1992, **27**, 1245–1249.
11. Yoshikawa, Y. and Uchino, K., Chemical preparation of lead-containing niobate powders. *J. Am. Ceram. Soc*., 1996, **79**(9), 2417–2421.
12. Ng, W. B., Wang, J., Ng, S. C. and Gan, L. M., Synthesis and dielectric characterization of lead magnesium niobate from precipitation and freeze-drying methods. *J. Mater. Chem*., 1998, **8**(10), 2239–2244.
13. Gupta, S. M. and Kulkarni, A. R., Dielectric and microstructure studies of lead magnesium niobate prepared by partial oxalate route. *J. Eur. Ceram. Soc*., 1996, **16**, 473–480.
14. Gupta, S. M., Harendranath, C. S. and Kulkarni, A. R., Synthesis and characterization of lead magnesium niobate having exceptionally high dielectric constant. *Ceram. Int*., 1997, **23**, 191–196.
15. Chaput, F., Boilot, J. P., Lejeune, M., Papiernik, R. and Hubert-Pfalzgraf, L. G., Low-temperature route to lead magnesium niobate. *J. Am. Ceram. Soc*., 1989, **72**(8), 1355–1357.
16. Nagakari, S., Kamigaki, K. and Nambu, S., Dielectric properties of sol-gel derived $Pb(Mg_{1/3}Nb_{2/3})O_3$–$PbTiO_3$ Thin Films. *Jpn. J. Appl. Phys*., 1996, **35**, 4933–4935.
17. Guo, H. K., Tang, X. G., Zhang, J. X., Shan, S. W., Wu, M. M. and Luo, Y. J., Preparation and dielectric properties of PMN–PT ceramics. *J. Mater. Sci. Lett*., 1998, **17**, 1567–1568.
18. Wang, D. M., Wang, J., Ng, S. C. and Gan, L. M., A sol-gel derived 0.9 $Pb(Mg_{1/3}Nb_{2/3})O_3$–$0.1PbTiO_3$ ceramic. *J. Mater. Res*., 1999, **14**(2), 537–545.
19. Narendar, Y. and Messing, G. L., Seeding of perovskite lead magnesium niobate crystallization from Pb–Mg–Nb–EDTA Gels. *J. Am. Ceram. Soc*., 1999, **82**(7), 1659–1664.
20. Jiwei, Z., Bo, S., Liangying, Z. and Xi, Y., Preparation and dielectric properties by sol-gel derived PMN–PT powder and ceramic. *Mater. Chem. Phys*., 2000, **64**, 1–4.
21. Beltrán, H., Cordoncillo, E., Escribano, P., Carda, J. B., Coats, A. and West, A. R., Sol-gel synthesis and characterization of $Pb(Mg_{1/3}Nb_{2/3})O_3$ (PMN) ferroelectric perovskite. *Chem. Mater*., 2000, **12**, 400–405.
22. Carvalho, J. C., Paiva-Santos, C. O., Zaghete, M. A., Oliveira, C. F., Varela, J. A. and Longo, E., Phase analysis of seeded and doped $Pb(Mg_{1/3}Nb_{2/3})O_3$ prepared by organic solution of citrates. *J. Mater. Res*., 1996, **11**(7), 1795–1799.
23. Cheng Ho, J., Liu, K. and Lin, I., Synthesis of $Pb(Mg_{1/3}Nb_{2/3})O_3$ perovskite by an alkoxide method. *J. Mater. Sci*., 1995, **30**, 3936–3943.
24. Kim, B. H., Ueda, K., Sakurai, O. and Mizutani, N., Synthesis of $Pb(Mg_{1/3}Nb_{2/3})O_3$ powder by the spray pyrolysis with ultrasonic atomizer. *J. Ceram. Soc. Jpn. Int. Ed*., 1991, **100**, 258–261.
25. Lukasiewicz, S. J., Spray-drying ceramic powders. *J. Am. Ceram. Soc*., 1989, **72**(4), 617–624.
26. Johnson, D. W. Jr., Innovations in ceramic powder preparation. In *Ceramic Powder Science*, ed. G. L. Messing, K. S. Mazdiyasni, J. W. McCauley and R. A. Haber. American Ceramic Society, Westerville, OH, 1987, pp. 3–19.
27. Lejeune, M. and Boilot, J. P., Formation mechanism and ceramic process of the ferroelectric perovskites: $Pb(Mg_{1/3}Nb_{2/3})O_3$ and $Pb(Fe_{1/2}Nb_{1/2})O_3$. *Ceram. Int*., 1982, **8**(3), 99–103.
28. Villegas, M., Moure, C., Duràn, P., Fernandez, J. F., Samardzija, Z. and Kosec, M., The role of PbO on the sintering behavior and microstructural development of $Pb(Mg_{1/3}Nb_{2/3})O_3$ based relaxors. *Key Engineering Materials*, 1997, **132–136**, 1076–1079.